# Energy transduction in the bacterial flagellar motor

## Effects of load and pH

Shahid Khan, Michaela Dapice, and Imran Humayun

Departments of Anatomy and Structural Biology & Physiology and Biophysics, Albert Einstein College of Medicine, Bronx, New York 10461

ABSTRACT The effect of load and pH on the relation between proton potential and flagellar rotation has been studied in cells of a smooth-swimming *Streptococcus* strain. The driving potential, speeds of free-swimming bacteria, and rotation rates of bacteria tethered to glass by a single flagellum were measured. The relation between rotation rate of tethered bacteria and potential was remarkably linear up to nearly −200 mV. The relation between swimming speed and potential exhibited both saturation and threshold, as previously observed in other species. The form of these relations depended on pH. The equivalence of the electrical and chemical potential components of the proton potential in enabling swimming depended on the voltage. Our observations may be most simply accommodated by a kinetic scheme that links transmembrane proton transits to a tightly coupled work cycle. The properties of this scheme were elucidated by computer simulations of the experimental plots. These simulations indicated that the protonable groups that participate in the rate limiting reactions have a fractional electrical distance between three-fourths to all of the way toward the cytoplasm with a corresponding mean proton binding affinity of $10^{-7.3}$–$10^{-7.0}$ M, respectively.

## INTRODUCTION

The rotation of bacterial flagella (Berg and Anderson, 1973) is energized by transmembrane ion gradients (Manson et al., 1977; Hirota and Imae, 1983). Bacterial flagellar motors are presently the subject of intense structural (reviewed by Macnab and DeRozier, 1988), chemical (reviewed by Stewart and Dahlquist, 1987), and biophysical (reviewed by Khan, 1988) study.

The basal structures of flagella, thought to serve as motor components, abut onto the cytoplasmic membrane. The structures are known, thus far, to include (*a*) a stack of discs, contiguous with the hook and filament, which may be isolated and purified (DePamphilis and Adler, 1971; Dimmit and Simon, 1971) and (*b*) rings of intramembrane particles which have only been observed in situ (Khan et al., 1988). Several protons act in synchrony (Khan et al., 1985) to power multiple force-generating units (Blair and Berg, 1988); but the structural identity of these units and mechanism of their function is not known. Models for the mechanism have been proposed (eg., Lauger, 1977; Oosawa and Masai, 1982; Berg and Khan, 1983; Mitchell, 1984) based on quantitative analyses of the dependence of rotation on the driving ion potentials and clues obtained from physico-chemical manipulations such as changes of temperature or isotope (Khan and Berg, 1983). Some of these models have been developed analytically (Oosawa and Hayashi, 1986; Lauger, 1988; Meister et al., 1989).

Experimentally, the relationship between heat and work in molecular motors may be approached by study and characterization of two fundamental relations: (*a*) the relation between motor speed and driving potential and (*b*) the relation between motor speed and force. Since the demonstration of energization of flagellar motors by proton gradients (Manson et al., 1977), quantitative measurements of the relationship between potential and speed have been made by a number of laboratories, but most extensively in "tethered" cells of *Streptococcus* by Berg's laboratory (Manson et al., 1980; Berg et al., 1982; Khan and Berg, 1983; Conley and Berg, 1984; Khan et al., 1985; Meister and Berg, 1987). Tethered cells are cells stuck to glass by a single flagellum so that the flagellar motor powers the rotation of the whole cell. In this high load regime the running torque is indistinguishable from the torque obtained at stall (Berg and Turner, 1979; Manson et al., 1980; Meister and Berg, 1987). In starved cells energized by jumping medium potassium or pH, tethered cell rotation increases linearly with the estimated Nernst potentials up to ~ −85 mV (Khan et al., 1985). Studies of the external pH dependence of glycolyzing tethered cell rotation (Manson et al., 1980; Meister and Berg, 1987) suggest that the linear relation is maintained up to at least −150 mV.

In other species, driven either by proton (*Bacillus*

Address correspondence to Dr. Khan.



0006-3495/90/04/779/18 $2.00

*subtilis* [Khan and Macnab, 1980; Shioi et al., 1980]) or sodium (*Bacillus firmus* RAB [Sugiyama et al., 1988]) gradients, the relation between potential and speed is markedly nonlinear, in contrast to *Streptococcus*. This variation could be due to species differences. However, all of these measurements, with one exception (Shioi et al., 1980), were made on swimming rather than tethered cells. Recently, Lowe et al. (1987) made measurements of bundle rotation in swimming cells of *Streptococcus* and showed that in this geometry flagellar motors rotated at high speeds and negligible torque, in contrast to the tethered case. The possibility arises that the different relations obtained are due to differences in frictional geometry and the operating load on the motor.

In this study we determined the relation between flagellar motor speed and the proton potential in cells of the smooth swimming *Streptococcus* strain V405197 and analyzed the changes effected by load and pH. Our study comprised 3 parts. (*a*) We repeated previous measurements (Manson et al., 1980; Meister and Berg, 1987) on glycolyzing tethered cell rotation, but in addition made measurements of the electrical and chemical proton potential components. The potentials imposed upon artificial energization of starved cells were also measured and their decay estimated. These measurements allowed determination of the speed-potential relation beyond $-85$ mV to $\sim -200$ mV and enabled comparison between artificially energized and glycolyzing cells. (*b*) We assessed the effect of external load on the relation between motor speed and potential by parallel measurement of free-swimming and tethered cells. (*c*) We assessed the effect of pH by manipulating cytoplasmic pH in starved cells, followed by energization at different pH's. In particular we compared, at the high motor speeds obtained in swimming cells, the pH dependence of saturation of the speed-potential relation and the equivalence between the electrical and chemical potential components.

To relate our measurements to the parameters that determine the speed-potential relation, we have outlined and analyzed a minimal kinetic scheme for transmembrane transit of the energizing protons and the motor work cycle. The assumptions implicit in this treatment are detailed and related to recent analyses of motor models (Lauger, 1988; Meister et al., 1989). Our observations are most simply consistent with a single cycle, saturation of motor speed under our experimental conditions being produced by voltage insensitive reactions intrinsic to the work cycle. Simulations of the experimental situations indicate that the protonable groups that participate in the rate-limiting reactions have a mean binding constant of $10^{-7.3}$–$10^{-7.0}$ M, corresponding to a fractional electrical distance between three-fourths and all of the way toward the cytoplasm, respectively.

## MATERIALS AND METHODS

### Materials, media, and cell preparation

Valinomycin (Sigma Chemical Co., St. Louis, MO) was used at 2 μg/ml final concentration, usually obtained as a 1:500 dilution from a 1-mg/ml methanolic stock solution. Prosil-28 (Thomas Scientific, Philadelphia, PA) was stored dessicated. Silicone oil (Aldrich Chemical Co., Milwaukee, WI) and n-octane (Sigma Chemical Co.) were used as a 96:4 mixture. Methylamine and benzoate ($Na^+$ salt), both from Sigma Chemical Co., were used to clamp the pH. $^3$H-tetraphenylphosphonium ($^3$H-TPP$^+$) was a gift from Dr. H. R. Kaback. Other radiochemicals used were $^3$H-$H_2O$ and $^{14}$C-inulin (Amersham Corp., Arlington Heights, IL), $^{14}$C-dimethylozalidodione ($^{14}$C-DMO), $^{14}$C-methylamine (American Radiolabelled Chemicals, St. Louis, MO), $^{86}$rubidium, and $^{14}$C-benzoic acid (New England Nuclear Research Products, Wilmington, DE).

*Streptococcus* V405197, a smooth swimming mutant derived from *Streptococcus* V4051 (Berg et al., 1982), was a gift of Dr. H. C. Berg. Cells were cultured in KTY medium (Manson et al., 1980). Single colony isolates were picked off KTY agar plates, tethered, and checked for phenotype (clockwise rotation alone when energized by acid pH shifts and counterclockwise rotation alone when energized by alkaline pH shifts), before being rapidly frozen in KTY plus 1% DMSO and stored at −80°C. Innocula were made into KTY media and the cells grown in midlogarithmic phase on a shaking water bath at 35°C. They were washed thrice with buffer A (100 mM sodium phosphate, 200 mM KCl, 0.1 mM EDTA, pH 7.5) and stored on ice. For artificially energized cell studies, the cells were treated with valinomycin, then incubated for half an hour at room temperature. For studies involving energization with glucose, both valinomycin-treated and untreated cells were used.

For tethering, cells were sheared by passage back and forth between two 5-ml syringes (18 gauge needles), washed once with buffer A, then incubated between 0.5 and 1 h on prosil-clad, 12-mm diam coverslips. Coverslips, cleaned in acetone followed by nitric acid, were stored in double-distilled water before being prosil coated. They were coated by being dipped in 5% prosil-28 solution for 15–30 s, rinsed by dipping in succession into two beakers of double-distilled water and dried in a 100°C oven 1–2 h before use.

### Motility measurements

The cells were monitored at ambient temperature in a stainless steel, observation flow cell, that has been described (Berg and Block, 1984). The coverslips served as detachable top windows for the cell, being fixed on with grease (Apiezon H). Lack of rotation of the tethered cells was used to confirm that the population was deenergized. For swimming speed measurements, unsheared bacteria were energized by dilution into buffer A containing 0.2% glucose, or artificially energized by dilution into buffer B (100 mM sodium phosphate, 200 mM NaCl, 0.1 mM EDTA, pH 7.5) or a buffer A/B combination at acid pH. Tethered cells were energized by flow through of these media. 10 s operation of a Gilson minipuls II pump (Rainin Corp., Woburn, MA) positioned at the output side of the cell, at a flow rate of 2 ml/min, was sufficient for exchange of the flow cell contents. Additional flow through of buffer did not increase rotation of the energized cells. Swimming and/or tethered cell measurements were not begun until ~10 min after introduction of glucose to ensure that the bacteria had reached metabolic steady state.

Simultaneous measurements of swimming speed and tethered cell rotation were made by drawing unsheared bacteria through the observation cell containing tethered cells. Another limb of tubing connected the

solution reservoirs directly to the pump, allowing flow to bypass the cell. Flow of media through the observation cell was initiated or stopped by flipping a three-way valve (LV3; Pharmacia Fine Chemicals, Piscataway, NJ) to channel flow through the flow cell or bypass limbs, with the pump kept in operation. For observations of artificially energized swimming motility, starved cells in buffer A were mixed with buffer B, defined volumes of cell suspensions in buffer A being pipetted into a milliliter of buffer B in a conical tube, and vortexed. The delay between energization of the swimming cells and measurements of their speeds was set by the length of tubing between mixing arrangement and cell, and the flow rate. It typically took ~10 s for the cells to enter the flow cell. This meant that the tethered cells were energized 10–15 s later than the swimming cells. At high potentials, tethered cells were measured 10–15 s out of phase with the swimming cells to correct for the rapid decay. For calibration of the imposed potassium diffusion potentials and pH shifts, the observation cell was replaced by flat combination pH (476551; Corning Medical, Medfield, MA) and potassium/reference electrodes (93-19/90-01; Orion Scientific Instruments Corp., Pleasantville, NY) encased in custom-made, flow-through chambers with volumes equal to the volume of the observation cell, ~50 μl. In some experiments, tethered cells or swimming cells alone were studied. In some tethered cell experiments, starved cells were first energized by a 1/20 shift of $K^+$ from 200 to 10 mM, then shifted to a higher potential either by change of pH or external $K^+$ for a few (<10) seconds before being downshifted back. For any given cell, the rotation rate at the higher potential was normalized by the rate obtained at 10 mM $K^+$.

Experiments were videotaped on a videorecorder (NV-8950; Panasonic) using a DAGE-MTI series 68 ultricon video camera, with adjustable black level and gain, coupled via a video zoom lens (Nikon Inc., Garden City, NY) to a Nikon Optiphot microscope operating in the bright field mode. Magnification was 600. Tethered cell rotation was analyzed manually by slow playback off line. A For-A, time-date generator, interposed between the camera and recorder, facilitated the analysis. Swimming cell speeds were analyzed manually or by computer. Computer assisted analysis utilized commercially available EV 3000 software (Motion Analysis Inc, Santa Rosa, CA); linear velocity and rate of change of direction operators were used for velocity measurement as described (Sundberg et al., 1986). The computer was scaled for distance by a videotaped image of a micrometre grid at the same magnification as that used for the experiments. Speeds obtained both manually and by computer on a selected data set were checked for identity.

## Radiolabeled measurements of membrane potential and pH gradients

The proton potential, $\Delta p$, is defined

$$\Delta p = \Delta\Psi - (2.3\ RT/F) \log (H_{ext}/H_{cyt}),$$

where $H_{ext}$ is the proton activity in the external medium, $H_{cyt}$ is the proton activity in the cytoplasm, $\Delta\Psi$ is the electrical potential difference between the inside and outside of the cell, log $\{H_{ext}/H_{cyt}\}$ is the transmembrane pH gradient, $\Delta$pH, $R$ is the gas constant, $F$ the Faraday and $T$ the temperature.

For measurement of pH gradients, $^{14}$C-benzoate (0.2 uCi/ml; sp· act 50 mCi/mmol) and $^{14}$C-methylamine (0.2 uCi/ml; sp· act 55 mCi/mmol) were used in the acidic and alkaline pH range, respectively. For measurements in the acidic pH range ($^{14}$C-benzoate or $^{14}$C-DMO), flow dialysis was necessary because consistent underestimates of pH gradients were obtained upon centrifugation through silicone oil. This was not the case for alkaline pH ($^{14}$C-methylamine) measurements, a finding also made by others (Tokuda and Unemoto, 1982). We used $^{14}$C-benzoate, because of its greater sensitivity (Kihara and Macnab, 1981) but checked that both it and the nonphysiological $^{14}$C-DMO gave similar values. For measurements of membrane potential we chose the lipophilic cation, tetraphenylphosphonium ($^3$H-TPP$^+$)(sp. act; 2.5 mCi/mmol), and $^{86}$Rb (sp. act; 400 mCi/mmol). The need for measurement in valinomycin untreated cells, as well as its fast uptake (Khan, 1980), made $^3$H-TPP$^+$ the probe of choice. To guard against artifacts (Kashket, 1985) we calibrated the probes against the estimated Nernst potentials obtained upon energization of starved cells and against each other.

A typical flow dialysis record is shown in Fig. 1 (*left*). Experiments

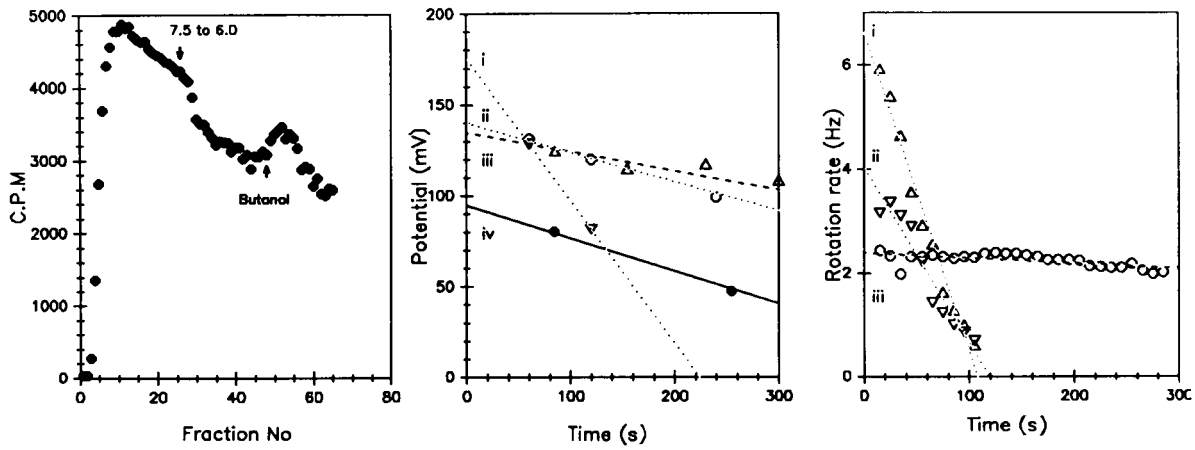


FIGURE 1 Raw data from flow dialysis, silicone oil centrifugation, and tethered cell experiments. (*Left*) Flow dialysis record of $^{14}$C-benzoate uptake. The pH was shifted from pH 7.5 to 6.0 by HCl addition. (*Center*) Silicone-oil/n-octane centrifugation data of $^{86}$Rb, $^3$H-TPP, and $^{14}$C-methylamine uptake. Upon energization (zero time), imposed $K^+$ diffusion potentials, estimated from the Nernst equation were −176.5 ($^{86}$Rb, *i*) and −132.3 ($^{86}$Rb, *ii*; $^3$H-TPP, *iii*) mV. Alkaline shift of pH from 7.5 to 8.5 was monitored by $^{14}$C-methylamine uptake (*iv*). (*Right*) Tethered cell rotation data. Energization (zero time) at imposed $K^+$ diffusion potentials, estimated from the Nernst equation, of −195 mV (*i*), −176.5 mV (*ii*), and −76.5 mV (*iii*). Linear best fits to the data are shown.

were started by addition of $^{14}$C-benzoate to 0.8 ml of buffer A + cells ($3 \times 10^{10}$/ml) in the upper chamber of a 1-ml flow dialysis cell (Bel-Art H40270); buffer A being pumped through the bottom chamber by the Gilson minipuls II at 4 ml/min. The two chambers were separated by a dialysis membrane (Spectrapor I, MW cut-off 6,000–8,000), a Gilson FC-80 K fraction collector being used to collect half-minute fractions. The volume of acid added so as to shift pH to 6.0 was determined by prior titration on an equivalent volume of cell suspension. Slopes before acid (fractions 15–27), after acid (fractions 33–45), and after butanol (fractions 55–65) addition were determined by linear regression. Fractions 30 and 45 corresponded to times of acid and butanol addition, respectively. The vertical displacements between the regression lines at fraction 30 and 45 indicated the amount of label taken up by acid and released by butanol addition respectively. The $\Delta$pH was calculated from these values as detailed in Ramos et al. (1976). The final cell density was between 1 and $3 \times 10^9$/ml. Note that comparison of the slopes of the segments obtained before acid and after butanol addiction indicates presence of a small $\Delta$pH in the deenergized cells at pH 7.5.

Representative records from the silicone oil centrifugation experiments on artificially energized cells are shown in Fig. 1 (*center*). Cells, treated with valinomycin and starved in buffer A, were energized by being pipetted into a beaker containing stirred buffer B and $^3$H-TPP$^+$ (1 $\mu$M final concentration) or $^{86}$Rb. The initial Nernst potential was estimated from the dilution factor for $K^+$. 0.2 ml aliquots were withdrawn at periodic intervals and centrifuged through a 96:4 mixture of silicone oil/n-octane (Conley and Berg, 1984). 0.1 ml of the supernatant was withdrawn for counting. The remainder of the supernatant fraction and the oil were removed by suction. The Eppendorf tube bottoms containing the pellets were clipped and dropped into scintillation vials. At the end of the experiment, 5% butanol (Guffanti et al., 1987) was added to the beaker and aliquots collected for estimation of the background uptake. In the case of $^{14}$C-methylamine uptake, an identical protocol was followed. In this case the pH difference was imposed by pipetting the cells into buffer A at an alkaline pH and the final pH obtained determined using a pH electrode.

The total water in the pellets obtained by such centrifugation was determined in experiments employing $^3$H-$H_2O$ (0.5 $\mu$Ci/ml). The excluded water was estimated by use of $^{14}$C-inulin (0.5 uCi/ml; sp. act 9 mCi/mmol). The difference gave the internal cell water in the pellet. This was normalized to a standard optical density. Optical density of cell suspensions was measured at 600 nm in a Spectronic 20 spectrophotometer (Bausch and Lomb Inc., Rochester, NY). We determined that one $OD_{600}$ unit corresponded to $3.6 \times 10^9$ cells/ml and 1.38 $\mu$l internal cell water/milliliter. The intracellular cell water was taken to be 60% of that value. This fraction was obtained in studies (Kashket and Barker, 1977; Bakker and Mangerich, 1981) on other *Streptococci* with radiolabeled compounds that penetrate the cell wall but not the cytoplasmic membrane, such as $^{14}$C-sorbitol. Because the ionic strength of the buffers was comparable to that of the cytoplasm, activity coefficients were not explicitly taken into account. The radioactivity was assayed in a scintillation counter (LS8100; Beckman Co., Palo Alto, CA), with Aquasol-2 as scintillant. $^{86}$Rb was counted using energy window settings used for $^{32}$P.

At moderate potentials, similar values were reported by $^3$H-TPP$^+$ and by $^{86}$Rb. Up to $-135$ mV, the imposed potential decayed gradually as measured by cation uptake. Above $-135$ mV, decay became precipitous. Tethered cell rotation followed a similar pattern. Three representative traces are shown in Fig. 1 (*right*). 10 cells were analyzed for each. For each cell, the mean rotation rates for successive 10 s intervals were computed. For each interval, the mean rotation rate obtained for the population was plotted. The decay of the membrane potential (as estimated by $^3$H-TPP$^+$ and $^{86}$Rb uptake) and that of tethered cell rotation showed good agreement and could be approximated as being linear. There was good correspondence between the estimated Nernst potentials and the initial potentials as obtained by back extrapolation

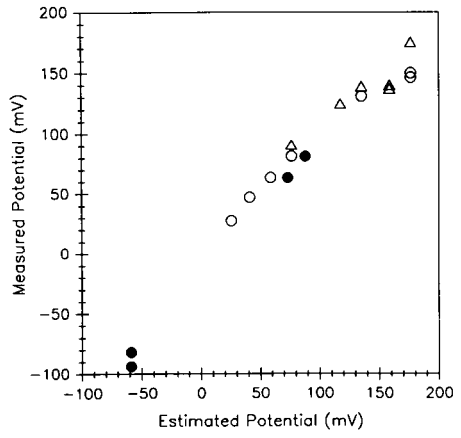


FIGURE 2 Comparison of estimated and measured imposed potentials in artificially-energized cells of *Streptococcus* V405197. Membrane potential was monitored by $^{86}$Rb (△) and $^3$H-TPP (○) uptake and $\Delta$pH (●) by $^{14}$C-benzoate (acid shifts) and $^{14}$C-methylamine (alkaline shifts) uptake. Estimated initial potentials were calculated from the Nernst equation and the known changes in external $K^+$ or pH. Measured initial potentials were estimated by linear back extrapolation (Fig. 1).

from the measured values (Fig. 2). At potentials above $-135$ mV, both the accuracy of the backextrapolation as well as match of the measured potential to the artificially energized motility suffered due to the precipitous decay (trace *i*, Fig. 1 [*center*]; trace *i* and *ii*, Fig. 1 [*right*]) and the correspondingly fewer data points. Beyond dilutions of >1:1,000, decay became much too severe to allow measurement. Upon acid pH jumps, we observed that cells, when shifted from pH 7.5 to pH 6.0 or 6.25, spun stably for many minutes, allowing measurement by flow dialysis, but not when shifted from pH 7.5 to 6.5 when they stopped within a minute or so. Linear best fits to the electrical (up to $-140$ mV) and pH gradient data indicated that starved, deenergized cells had a residual $\Delta\Psi$ of $\sim -9$ mV ($s \cdot e = 4$) and a residual (2.3 $RT/F$)$\Delta$pH of $\sim$19 mV ($s \cdot e = 4$) consistent with the NMR measurements of Conley and Berg (1984).

Our studies of artificially energized motility took into account the observed decay patterns. Both tethered cell rotation and swimming speed measurements were made 15–45 s after energization and matched with values of the potential 30 s after energization, as obtained by back extrapolation. Measurements were sometimes made in two or three windows of 5 s each so as to give an indication of the decay.

We do not understand the observed decay patterns in the artificially energized experiments, particularly at acid pH. Decay kinetics are complicated by the probable presence of a $H^+/Na^+$ antiporter (Khan, unpublished results; Meister, 1987). For a 1:20 dilution ($-76.5$ mV $\Delta\Psi$), we determined that the decay of the imposed potential, supplied largely or entirely as $\Delta\Psi$, was governed predominantly by dissipation of the imposed $\Delta\Psi$, rather than buildup of an opposing (2.3 $RT/F$)$\Delta$pH. We estimated net acidification by $^{14}$C-methylamine uptake. The final (2.3 $RT/F$)$\Delta$pH was $-28$ mV ($s \cdot e = 8$) compared with the residual $-19$ mV before energization. A $H^+/Na^+$ antiporter if present could act, in sodium buffers, to prevent buildup of a $\Delta$pH as observed.

The measurements on glycolyzing cells followed the calibration procedures on artificially energized cells detailed above, with the difference that jumps of pH or dilutions of buffer potassium were omitted. In the glycolyzing cell measurements, the probes were added to cells in buffer A (+0.2% glucose), already at the desired pH and concentration for ~10 min.

## Simulations and data analysis

Programs were written in GW-Basic to run on an AT&T 6300 IBM compatible Personal Computer. Commercially available software (Sigmaplot, Jandel Inc., Sausalito, CA; Asystant, Macmillan Software, New York, NY) was utilized to provide fits to the data.

## RESULTS

### Motility in glycolyzing cells of *Streptococcus* V405197

The proton potential was varied either by changing the chemical potential, $(2.3\ RT/F)\Delta pH$, or the electrical potential, $\Delta\Psi$. We changed $\Delta pH$ by shifting the pH of the buffer. We changed $\Delta\Psi$ by addition of valinomycin and combined such a manipulation with changes of $\Delta pH$.

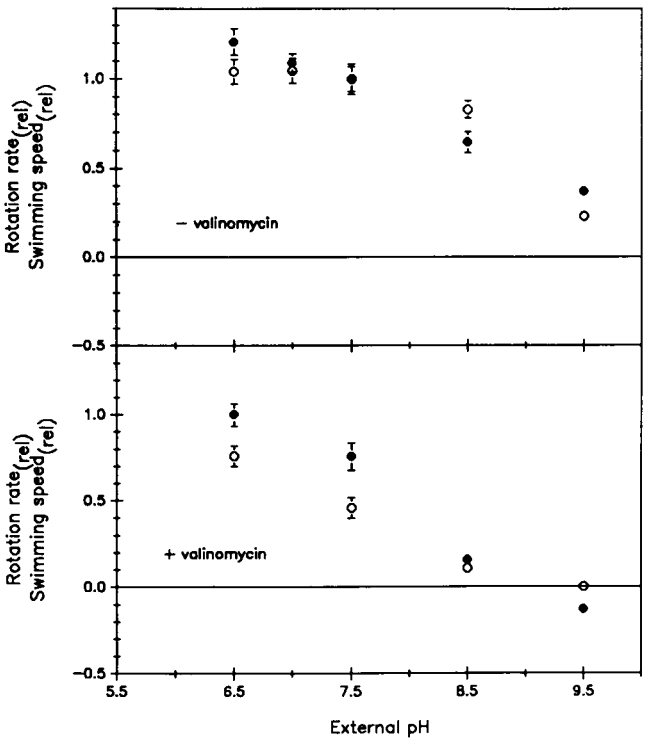


FIGURE 3 Motility in glycolyzing *Streptococcus* V405197 as a function of external pH. (*Top*) Cells not treated with valinomycin. (*Bottom*) Cells treated with 2 μg/ml valinomycin. Parallel measurements of tethered (●) and free-swimming cells (○) were made. Two independent experiments are represented for each treatment. A total of 15 tethered cells were measured for each case. For each cell, rotation rates at the different pH values were normalized by its rate at pH 7.5. The absolute mean rate obtained at pH 7.5 in valinomycin-treated tethered cells was scaled relative to the corresponding mean rate for untreated cells (6.5 Hz). Swimming data points represent 30–50 paths each. These speeds were normalized by the untreated cell population mean speed at pH 7.5 (18 μm/s).

Parallel measurements of tethered cell rotation rate and free-swimming cell speed were made to eliminate variations from culture to culture. These measurements are shown in Fig. 3.

Upon shift from pH 6.5 to 6.0, untreated cells sometimes increased and sometimes decreased speed. Such culture to culture variations might be responsible for the variability in reports documenting changes in tethered cell rotation rate upon shift from pH 7.5 to 6.0 (compare Fig. 10 of Manson et al., 1980 with Fig. 6 of Meister and Berg, 1987). Nonspecific damage at pH 6.0 may account in part for such variation. Accordingly, we restricted study of glycolyzing cells to pH 6.5 and above.

Tethered cell rotation increased upon acidification in all cases over the range studied. The increase was gentler in untreated cells for shifts in the acid range. When the pH was shifted from 7.5 to 9.5 in valinomycin-treated tethered cells, the cells reversed rotation sense and maintained stable speed in the reversed sense for >10 min.

For any given pH shift, the change in free-swimming cell speed differed depending on whether valinomycin-treated or untreated cells were being studied. In particular, untreated cells did not increase swimming speed when shifted from pH 7.5 to 6.5, whereas treated cells increased speed. Over the pH range 9.5–8.5, untreated cells increased swimming speed sharply, whereas treated cells remained largely immotile. In the absence of valinomycin, over the pH range 8.5–6.5, tethered cells increased rotation rate by >50%, whereas swimming cell speed increased by ~15%. Because the pH changes were the same in either case, the observed differences in swimming behavior had to be due to the different potentials obtained in the two (valinomycin-treated and untreated) conditions. Similarly, the observed differences in the behavior of tethered versus swimming cells had to be a result of their different frictional geometries.

### Proton potential in glycolyzing *Streptococcus* V405197

The $TPP^+$ measurements of electrical potential and the benzoate/methylamine measurements of pH gradients in glycolyzing cells are compiled in Table 1. Over the external pH range 6.0–9.0, *Streptococcus* V405197 maintains excellent pH homeostasis and a resting potential of ~ −130 mV. This potential is insensitive, within error, to changes of pH between 6.5 and 9.5. Upon treatment with valinomycin, the internal pH is maintained at a value of ~0.3 pH units more alkaline than in the absence of valinomycin, and homeostasis is not as stringent. The membrane potential decreases by ~ −60 mV and remains constant, within error, upon shifts of pH.

**TABLE 1 pH homeostasis in glycolyzing *Streptococcus***

| $pH_{ext}$ | $pH_{int}$ − valinomycin | $\Delta\Psi$ | $pH_{int}$ + valinomycin | $\Delta\Psi$ |
|---|---|---|---|---|
| 6.5 | 7.4 | −136 | 7.7 | −66 |
| 7.0 | — | −131 | — | — |
| 7.5 | — | −130 | — | −69 |
| 8.5 | 7.6 | −144 | 7.8 | −72 |
| 9.5 | 7.7 | −150 | 8.0 | −63 |

At a given external pH, $pH_{ext}$, the internal pH, $pH_{int}$, was determined from the measured ΔpH. At $pH_{ext}$ 6.5, ΔpH was measured by $^{14}$C-benzoate uptake using flow dialysis. At $pH_{ext}$ 8.5 and 9.5, ΔpH was measured by $^{14}$C-methylamine uptake using centrifugation through silicone oil. The ΔΨ was estimated from $^{3}$H-TPP$^{+}$ uptake, also by silicone oil centrifugation. Each measurement is the mean of duplicate experiments done on separate cultures. Culture to culture variations were greater than the variation in the estimates of ΔpH or ΔΨ within an experiment. In individual experiments, ΔpH or ΔΨ could be determined within 0.1 pH u (i.e., 6 mV). One estimate of the culture to culture variation was computation of the overall standard deviation (square root of the sum of the variances obtained for each measurement) for each measurement class. This was 0.25 pH units ($^{14}$C-benzoate ΔpH measurements), 0.2 pH units ($^{14}$C-methylamine ΔpH measurements), 15 mV ($^{3}$H-TPP$^{+}$ ΔΨ measurements [untreated cells]), and 7 mV ($^{3}$H-TPP$^{+}$ ΔΨ measurements [valinomycin treated cells]), respectively.

## Tethered and free-swimming cell speed as a function of the proton potential

The pooled measurements of motility and potential in artificially energized and glycolyzing cells are shown in Fig. 4.

For any given potential when glycolyzing cells were compared with artificially energized cells, lower speeds were obtained in the artificially energized case. This is due, in part, to buildup of a small ΔpH during deenergization as discussed above. For tethered cell rotation (Fig. 4 [*top*]) the discrepancy is small and would be largely accounted for upon appropriate correction for the (2.3 $RT/F$)ΔpH buildup. Valinomycin-treated glycolyzing cell swimming speeds showed better agreement with artificially energized cell speeds than untreated glycolyzing cell speeds (Fig. 4 [*bottom*]). Voltage could affect the rate of the reactions limiting motor speed. However, this is unlikely to be a major effect in the regime (~ −70 mV ΔΨ) being considered here because equivalent increases of membrane voltage or chemical potential produced equal changes of speed within error (Fig. 4 [*bottom*]). It remains possible that speeds obtained upon energization by delocalized bulk-phase potentials are lower than those obtained by glycolysis (Williams, 1988). However, given the random culture to culture variations and the systematic error caused by neglect of (2.3 $RT/F$)ΔpH buildup, the evidence, on balance, indicates that artificial energization by shifts of bulk-phase potentials is not significantly slower.

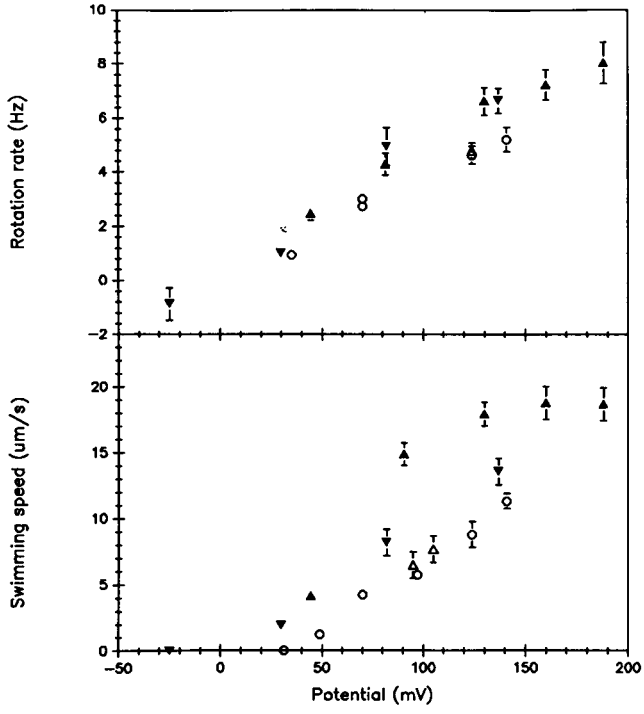


FIGURE 4 Motility as a function of energizing potential. (*Top*) Tethered cell rotation rate. (*Bottom*) Swimming cell speed. Composite of measurements on glycolyzing cells (▲), glycolyzing cells treated with valinomycin (▽), cells energized by imposition of ΔΨ (O), and ΔpH plus −76.5 mV ΔΨ (△). The data for glycolyzing cells from Fig. 3 are replotted as a function of the proton potential computed from the ΔΨ and ΔpH measurements listed in Table 1. Potentials for the artificially energized data were obtained by back extrapolation from $^{86}$Rb measurements to 30 s after energization (ΔΨ data alone). In the case of potentials involving ΔpH increments, values at 30 s were assigned by assuming decay rates corresponding to equivalent potentials comprised of ΔΨ alone. The data for artificially energized tethered cells are comprised of 20 cells for each case (ΔΨ alone or combined ΔΨ/ΔpH). The cells were initially energized by replacement of 200 mM by 10 mM K+ (−76.5 mV estimated Nernst potential). They were then shifted briefly (10 s) to a higher potential by flow through of buffer (swimming cells plus buffer in experiments involving parallel measurements of tethered cell rotation and swimming speed) at lower external $K^{+}$ or pH, then downshifted back to −76.5 mV ΔΨ by flow through of 10 mM $K^{+}$, pH 7.5 buffer. Each artificially energized swimming cell data point represents ~30 paths. Rotation rates and swimming speeds were normalized, then scaled, by the mean value obtained at −76.5 mV. Bars denote standard errors.

The relation between tethered cell rotation and potential was remarkably linear (Fig. 4 [*top*]), curving gently at the highest potentials. The relation between swimming speed and potential exhibited a distinct threshold. Saturation and threshold phenomena have been observed previously for free-swimming cells of other species (Khan and Macnab, 1980; Shioi et al., 1980). In these bacteria,

swimming speeds saturated regardless of whether the $\Delta\Psi$ or $\Delta$pH was incremented. This implies that the events limiting motor speed are insensitive to voltage and that there is a common step limiting rotation driven by electrical or chemical gradients because the same saturation speed is obtained in these two cases. In *Streptococcus*, at physiological pH 7.5, saturation was observed when $\Delta$pH was incremented in untreated, but not in valinomycin-treated, cells. As noted above, a small voltage dependence of the reactions limiting motor speed could underlie this difference. In any case, as documented below, at acid internal pH 6.25, saturation as a function of $\Delta\Psi$ was obtained.

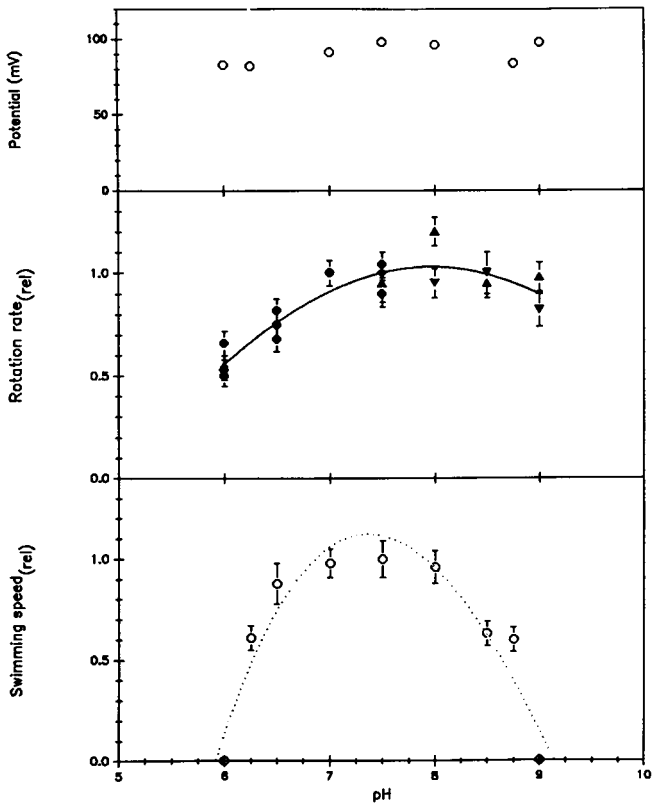


FIGURE 5 pH dependence of energization and motility in *Streptococcus* V405197. (*Top*) Imposed membrane potential as reported by $^{86}Rb$ uptake. Initial potentials, obtained by back extrapolation, are plotted. Each datum represents mean values from duplicate experiments. (*Center*) Tethered cell rotation. Experiments were done in buffer alone (▼; 25 cells), in buffer + 100 mM methylamine (▲; 20 cells), and in buffer + 25 mM benzoate (●; 40 cells). In all cases cells were first energized at pH 7.5, deenergized and shifted to the pH of interest, left for 30 min to allow equilibration, then energized. Speeds attained by the cells when energized at the pH of interest were normalized by division with the speeds obtained during the first energization at pH 7.5 so as to allow comparison between experiments. (*Bottom*) Swimming speed. Composite of multiple experiments on separate cultures. Speeds obtained at any given pH were normalized relative to the swimming obtained by equivalent energization at pH 7.5 which was always measured for the culture used. Each datum represents between 30 and 50 swimming paths. In all cases, cells were energized by shifting external $K^+$ from 200 to 10 mM. Bars denote standard errors. Best fit third-order polynomials to the motility data are shown.

## pH titration of tethered and swimming cell motility driven by a constant voltage

Fig. 5 shows the internal pH dependence of the imposed membrane potential, tethered cell rotation, and swimming cell speed. The internal pH was manipulated as described in Materials and Methods. The shifts of pH transiently energized the starved cells and they rotated. With time, typically within half an hour, the rotation stopped as deenergization occurred. The potential in cells deenergized after shifts of pH from 7.5 to 6.0 and 9.0 was between $-10$ and $-15$ mV (duplicate experiments for each pH value). Given electrochemical equilibrium, the opposing chemical potential, $(2.3\ RT/F)\Delta$pH, would be $\sim -10$–15 mV. This meant that the internal pH corresponded to the external pH to within 0.25 pH units. Consistent with these measurements, equilibration in the presence of benzoate or methylamine, reagents, which at high enough concentrations greatly reduce the $\Delta$pH (Kihara and Macnab, 1981), did not affect the pH dependence of tethered cell rotation rate (Fig. 5 [*center*]).

The membrane potentials generated by 1:20 dilution of cells in buffer A into buffer B were independent of pH and close to the estimated Nernst potentials, $\sim -76.5$ mV (Fig. 5 [*top*]). The slightly elevated values ($\sim -10$ mV) obtained probably compensated for a small residual $\Delta$pH present in the deenergized cells.

We found, as did Meister and Berg (1987), that tethered cells will not rotate at extreme pH values (i.e., pH 5.5 or 11.0) when energized in this fashion. We therefore examined the pH dependence of the motility parameters over a restricted pH range pH 6.0–9.0. Over the pH range 7.5–9.0, tethered cell rotation showed a weak pH dependence, as judged by the best fit third degree polynomial drawn (Fig. 5 [*center*]), but this was not significant given the associated error. Over the pH range 6.0–9.0, tethered cell rotation decreased at acidic values. At pH 6.0, rotation rates obtained upon energization were <50% of the rates obtained at pH 7.5. Fig. 5 (*top*) rules out the possibility that the decrease was due to the impaired generation of potential by valinomycin/$K^+$, but does not allow unambiguous interpretation. It could be that the decrease in tethered cell running torque ($\simeq$ stall torque [Meister and Berg, 1987]) observed at the low pH values is due to slippage, analogous to the decrease in isometric tension observed at high ATP levels in muscle fibers (Cooke and Bialek, 1979). Alternatively, there

could be pH-dependent changes in the number or efficiency of active force-generating units.

The pH dependence for swimming cell speed was sharper than that for tethered cell rotation (Fig. 5 [*bottom*]), particularly over the alkaline pH range. At pH 9.0, swimming motility could not be generated, whereas tethered cells spun at rates similar to that obtained when cells were energized at pH 7.5. The tethered cell measurements showed that motors are capable of maximal torque production over the entire alkaline pH range from 7.0 to 9.0. Thus, the observed decrease in swimming cell speed at alkaline pH could not be due to a decrease in the number or efficiency of force-generating units. Swimming motility also dropped at acidic pH. At pH 6.0, as at pH 9.0, no swimming motility could be generated.

## The effect of pH on the potential dependence of tethered cell rotation and swimming speed

We examined the potential dependence of tethered cell rotation and swimming speed at two extremes of the pH dependence curve (Fig. 5): pH 6.25 and 8.75. At these pH's, similar swimming speeds were obtained upon energization to an estimated −76.5 mV Nernst potential (Fig. 5 [*bottom*]). We concentrated on measurement and analysis of swimming behavior at high potentials (> −70 mV). At lower potentials, both the number as well as speed of the swimming cells decreased (data not shown). In addition, possible changes in bundle hydrodynamics at very low speeds rendered interpretation difficult.

As at pH 7.5, artificially energized motility at either 6.25 or 8.75 decayed rapidly above −140 mV. At the highest potential (~ −176 mV) imposed, motility had declined significantly in the first 30 s. As at pH 7.5 this was largely due to rapid decay of the imposed $\Delta\Psi$, as indicated by $^{86}Rb$ measurements of the $\Delta\Psi$ and $^{14}C$-methylamine measurements of the net $\Delta pH$ buildup (not shown). Observations on tethered and swimming cell motility were made immediately (between 15 and 45 s after energization). These measurements were related to the potential obtained 30 s after energization by back extrapolation from $^{86}Rb$ measurements. The net $\Delta pH$ buildup at either pH 6.25 or pH 8.75 was < −15 mV during deenergization of a −76.5-mV pulse of $\Delta\Psi$. At higher potentials, we measured an even smaller $\Delta pH$ buildup. Consequently, as at pH 7.5 (Fig. 4), this parameter was ignored in plots of the data (Fig. 6).

The potential dependence was quite different at these two pH values. At pH 6.25, saturation was obtained after ~ −100 mV (Fig. 6 [*bottom left*]). By contrast, swimming speeds continued to increase sharply at pH 8.75 over the entire potential range experimentally accessible to us. The best fit linear regression to the data (Fig. 6 [*bottom right*], $\Delta\Psi$ alone) upon back extrapolation to zero speed intercepted at a finite potential (not shown). Tethered cells rotated faster at pH 8.75 than at pH 6.25. As the potential was increased, rotation rates continued to increase at both pH's; but the slope of this increase was gentler at pH 6.25, decreasing at higher potentials (Fig. 6 [*top left*]). At pH 8.75 a remarkably linear curve was obtained (Fig. 6 [*top right*]). Thus, tethered cell rotation reflected, albeit to a modified degree, the striking differences between potential plots of the swimming speed.

## Kinetic equivalence of $\Delta\Psi$ and $\Delta pH$

We examined the kinetic equivalence of electrical and chemical potentials at pH 8.75 because this allowed imposition of a greater pH difference, $\Delta pH$, as compared with pH 7.5, where this equivalence had been studied previously (Manson et al., 1980; Berg et al., 1982; Khan and Berg, 1983).

We found, strikingly, that swimming motility could not be generated at pH 8.75, when the pH alone was shifted (−76.5 mV chemical potential). This was in marked contrast to the case for tethered cells, where similar speeds were obtained upon imposition of either a −76.5-mV chemical potential alone or an electrical potential alone. Earlier studies (Manson et al., 1977) had shown that starved cells "jiggled" (moved weakly or sporadically in place) when shifted from pH 7.5 to pH 6.5 or 5.5. They "twiddled" (jumped about vigorously) or ran (in the presence of chemoattractant, L-leucine) when a potassium diffusion potential was applied. Whereas, as well documented (Manson et al., 1980; Berg et al., 1982; Khan and Berg, 1983), similar tethered cell rotation rates at pH 7.5 were obtained upon imposition of an equivalent chemical or electrical potential alone. The differences in swimming behavior observed at pH 7.5 seemed, then, to be accentuated by the lower proton activity at pH 8.75.

We restricted study to imposition of $\Delta pH$'s in concert with $\Delta\Psi$. When the buffer pH was shifted from 8.75 to 7.5 or 7.25, this time in concert with a $K^+$ shift of 1/20 (−76.5 mV estimated $\Delta\Psi$), cells swam more vigorously than upon imposition of the $\Delta\Psi$ alone. Problems remained with assignment of a $\Delta pH$ value obtained over the period of the measurement. We could not measure the $\Delta pH$ decay directly. However, as at internal pH 7.5, we observed that decay as evidenced by tethered cell rotation was similar to the decay observed when an equivalent value of $\Delta\Psi$ was imposed. On this basis, over the period of the motility measurements (15–45 s), the potential obtained upon the combined $\Delta\Psi/\Delta pH$ shifts was assigned a value equal to that obtained upon an equivalent $\Delta\Psi$ shift

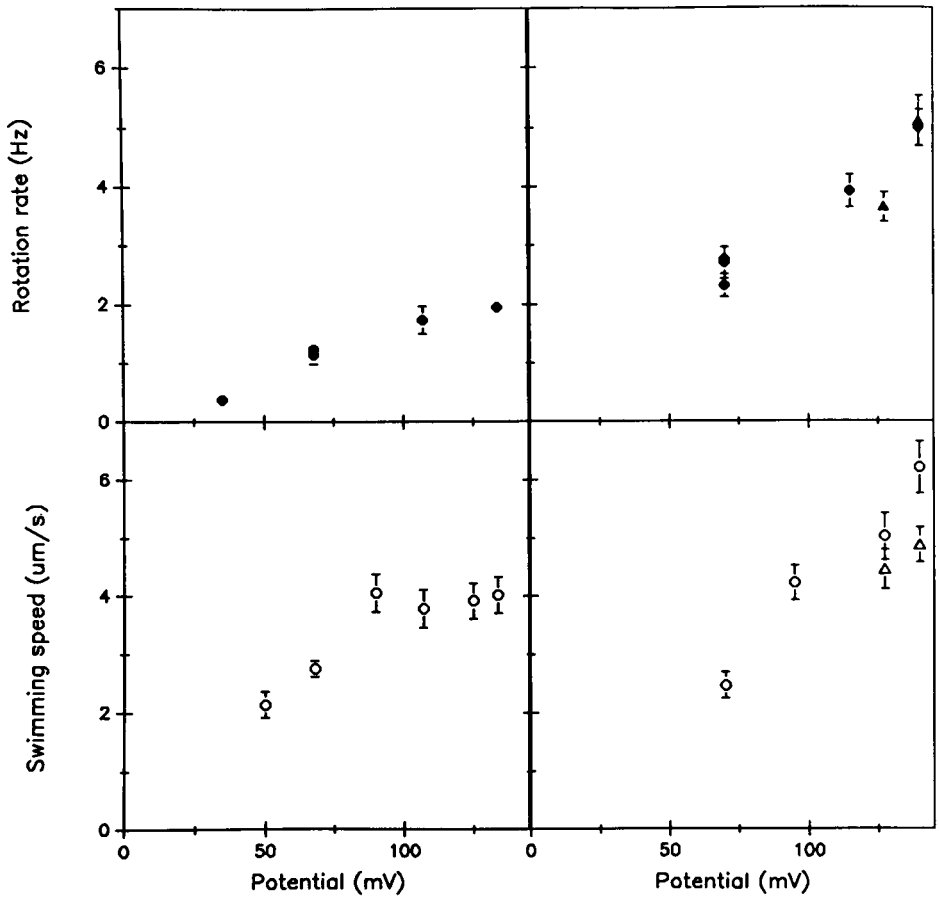


FIGURE 6 Potential dependence of tethered cell rotation (●, $\Delta\Psi$) [▲, $\Delta\Psi - (2.3\ RT/F)\Delta pH$]: (*Top left*) pH 6.25. (*Top right*) pH 8.75. Cells were energized by 76.5 mV by shifting external $K^+$ from 200 to 10 mM, shifted to a higher potential (lower $K^+$ or pH) for a few seconds, then downshifted back to 10 mM $K^+$. Speeds at the higher potential were then normalized to the mean speed obtained at 10 mM. Rotation of between 10 and 20 cells was measured for each potential value. Swimming cell speed (○, $\Delta\Psi$) [△, $\Delta\Psi - (2.3\ RT/F)\Delta pH$]: (*Bottom left*) pH 6.25 (*Bottom right*) pH 8.75. Experiments were carried out in triplicate for each potential, a total of 40–60 paths being measured for each value. For each culture, speeds obtained upon imposition of a −76.5-mV estimated Nernst potential were measured. The speeds obtained at the higher potential values were normalized by these speeds so as to allow comparison between cultures. The normalized speeds were scaled by multiplication with the absolute mean speeds obtained at −76.5 mV, and related to potentials obtained at times corresponding to the motility measurements, i.e., 30 s after energization. The potentials were obtained by back extrapolation from duplicate $^{86}Rb$ measurements (Fig. 1 [*center*]). Swimming and tethered cell motility was measured between 15 and 45 s after energization. Bars denote standard errors.

alone. The measurements obtained in each case are plotted together for tethered (Fig. 6 [*top right*]) and swimming (Fig. 6 [*bottom right*]) cells.

## ANALYSIS

### Kinetics of transmembrane transit of the protons energizing flagellar rotation

The minimal kinetic scheme that will suffice for description of the observed relations between motor speed and proton potential is shown in Fig. 7. The scheme is analyzed for the simplest case where transport of each proton produces an elementary displacement. For clarity, we consider a single force-generator motor. Because flagellar motors are comprised of independently acting force generators (Blair and Berg, 1988), extrapolation of our arguments to motors with the normal complement of force generators is straightforward.

The scheme depicts the sequence of reactions during transmembrane transit of the protons energizing flagellar rotation. Protons are transferred (reactions [1] and [6]) via channels from the adjacent bulk phases to groups,

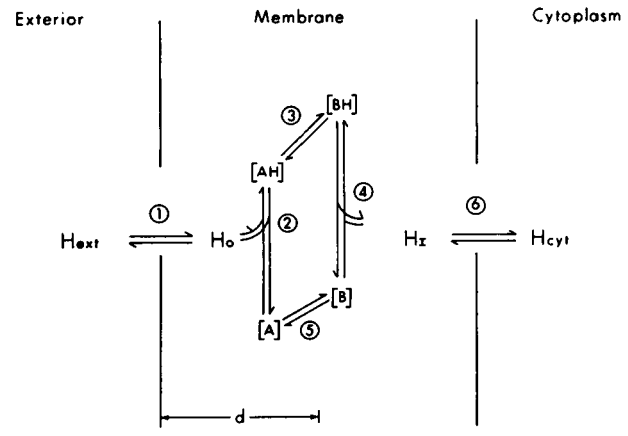


FIGURE 7 Transmembrane transit of protons energizing flagellar rotation: $H_{ext}$ = ion activity of the external bulk phase. $H_{cyt}$ = ion activity of the internal bulk phase. *Ho* = external ion activity of the energy coupling sites. *Hi* = internal ion activity at the energy coupling sites. *d* = fractional electrical distance. For constant electric field, $d = 0.5$ in the figure. In configuration [*A*] of the force generator, the group whose protonation/deprotonations coupled to force generation ("energy coupling site") is accessible to protons from the external bulk phase. In configuration [*B*] it is accessible to protons from the internal bulk phase. [*AH*] and [*BH*] are protonated forms of these configurations. One cycle of configurational transitions of the force generator ("work cycle") results in the transmembrane transit of one proton and a fixed elementary angular displacement of the flagellum. Rate constants for reactions involving transmembrane transfer of protons, reactions (1) and (6), are sensitive to voltage. Reactions of the work cycle ([2]–[5]) are postulated to be voltage independent, proceeding transverse rather than across the membrane. The rate constants of the energy coupling reaction, identified as (3), are modulated by the load.

protonations/deprotonations (reactions [2] and [4]) of which couple to force generation (reaction [3]). It would be expected that the rate constants of proton transfer reactions that proceed within and transverse to the membrane would be sensitive to voltage because charge movements within an electric field are involved. Thus, reactions (1) and (6) would be sensitive to voltage. Reactions (2)–(5), which comprise the work cycle, may or may not be sensitive to voltage. We explicitly assume that these reactions are insensitive to voltage. Our observations and those of others on the saturation of motor speed require the presence of voltage-insensitive reactions.

The nature of the force-generating transition (reaction [3]) is left unspecified. The transition could involve mechanical motion alone (e.g., stretch of an elastic linkage [Berg and Khan, 1983]), mechanical motion coupled to a change in conformational state (Eisenberg et al., 1980), or conformational transition between alternating states (Tanford, 1983). The analysis is not dependent on specifics of mechanism.

The work cycle is formalized most simply as a single cycle (Hill, 1977) in our scheme. Formulation of the work cycle as a single cycle indicates that coupling is assumed to be absolute (i.e., tight). Therefore,

$$(d\alpha/dt) = c(dH/dt), \quad (1)$$

where $(d\alpha/dt)$ is the angular displacement (in radians) per second, $(dH/dt)$ is the proton flux and the proportionality constant, $c = 2\pi/n$, where $n$ is the number of protons translocated per revolution. Motor frequency, $\upsilon = [(d\alpha/dt)/2\pi]$ Hz.

The voltage and the load determine which reactions limit the proton flux. Voltage will increase both the local activity of protons at the energy coupling sites *and* the rate constants of the transmembrane proton transfer reactions ([1] and [6]). Our observations at internal pH 8.75, namely that tethered cells spin equally well when energized by equivalent chemical or electrical potentials, whereas swimming cells in contrast do not translate when energized by a chemical potential, but do so when energized by an equivalent electrical potential, may be explained thus. At high load (i.e., in tethered cells), reaction (3) will be rate limiting. The local activities, *Ho* and *Hi*, will be in equilibrium with the bulk phase activities $H_{ext}$ and $H_{cyt}$, respectively. Equivalent rotation rates will be obtained when cells are energized by an equivalent electrical ($\Delta\Psi$) or chemical potential $[(kT/e) \cdot \log (H^1_{ext}/H^2_{ext})$, when external pH is changed from $H^1_{ext}$ to $H^2_{ext}]$, because the only effect of voltage in this case would be modulation of *Ho*, where $Ho = H_{ext} \cdot \exp(-\Delta\Psi \cdot e/kT)$ given fractional electrical distance, $d = 1$. At low load (i.e., in swimming cells) and zero voltage, reactions (1) or (6) or both will be rate limiting. Under this condition, the electrical and chemical potentials will no longer be equivalent because the imposed voltage will change both the local activities relevant for, and the rate constants of, the limiting reactions. Modulation of rate would depend on the voltage drop across the groups participating in these reactions and could be large given appropriate stereochemistry. However, as the voltage is increased the reactions would be accelerated to the stage where they cease to be limiting. The only effect of further increasing voltage would now be modulation of the local proton activities, *Ho* and *Hi*, as in the high load case and equivalence of the chemical and electrical potentials will depend only on *d* (see below).

The properties of our kinetic scheme relevant for analysis of our experimental observations may be worked through with minimal assumptions. We have already assumed that: (*a*) the work cycle is tightly coupled, (*b*) transport of one proton is coupled to an elementary displacement, and (*c*) the rate constants of the reactions comprising the work cycle are insensitive to voltage.

We assume further that: (*d*) the cycling states [*A*] and [*B*] have equal free energies and the states [*AH*] and

$[BH]$ have equal free energies. We consider a special case of nonisoenergetic cycling states later when we consider possible changes in proton binding affinities during cycling. Isoenergetic cycling states have been argued in the literature to be kinetically favorable for energy coupling (Tanford, 1983). Because there will be no free energy change during transitions between $[A]$ and $[B]$, the activation energy for both the forward and back transition will be the same. Thus, the rate constant for the forward transition $[A]$ to $[B]$, $k_{[A]-[B]}$ is the same as the back transition, $k_{[B]-[A]}$. It is also reasonable to assume that the activation energy for these transitions remains unchanged upon protonation. Thus,

$$kc = k_{[A]-[B]} = k_{[B]-[A]} = k_{[AH]-[BH]} = k_{[BH]-[AH]}.$$

(*e*) Our observations have centered on the changes in the speed-proton potential relation obtained at high voltage ($> -70$ mV) as a function of load, pH, and interconversion of the electrical and chemical proton-potential components. For simulations of these observations, we assume that, at voltages $> -70$ mV, the transmembrane proton transfers (reactions [1] and [6]) are in rapid equilibrium. Comparable increases in swimming speed were obtained when cells were energized by a combination of $\Delta\Psi$ and $(2.3\ RT/F)\Delta$pH as opposed to a $\Delta\Psi$ alone, at both internal pH 7.5 (Fig. 4 [*bottom*]) and 8.75 (Fig. 6 [*bottom right*]). These suggest that this assumption is largely, if not entirely, justified.

Consider, first, the motor speed proton-potential relation at zero load at a fixed fractional electrical distance, $d$. We consider variations in $d$ later in detail, but initially we assume a "proton well" ($d = 1$) as in earlier work (Khan and Berg, 1983). As derived in Appendix A, the proton flux, $(dH/dt)$, then, is

$$kc \cdot (Ho - Hi)/2\{[(Kd + Ho) \cdot (Kd + Hi)/Kd] + [kc/(ka \cdot Kd)][(2 \cdot Kd) + Ho + Hi]\}, \quad (2)$$

where $[kc/(ka \cdot Kd)]$ represents the ratio of the mechanical/proton dissociation reactions. $Kd$ is the equilibrium binding constant; $ka$ is the bimolecular proton binding rate constant. For the moment, $Kd$ is assumed to be the same for both configurations $[A]$ and $[B]$, but again this point is considered in detail later. Fig. 8 presents simulations of Eq. 2 for the speed-potential relation at pH 7.5 and the pH dependence, for varying ratios of $[kc/(ka \cdot Kd)]$. In Fig. 8, as in the following figures, relative speed is plotted because $v$ has been assumed proportional to $(dH/dt)$.

Comparison of Fig. 8 with Figs. 4 (*bottom*) and 5 (*bottom*) shows that the data do not discriminate strongly between whether work cycle protonations/deprotonations (reactions [2] and [4]) are in rapid equilibrium ($ka \cdot Kd \gg kc$) or rate limiting ($kc \gg ka \cdot Kd$). If the latter were true, the pH dependence curve will not decline noticeably upon acidification of internal pH from 7.5 to 6.0 (Fig. 8). As $Ho$ tends to infinity, Eq. 2 tends to $kc \cdot (ka \cdot Kd)/2\{[ka \cdot (Kd + Hi)] + kc\}$. The depen-

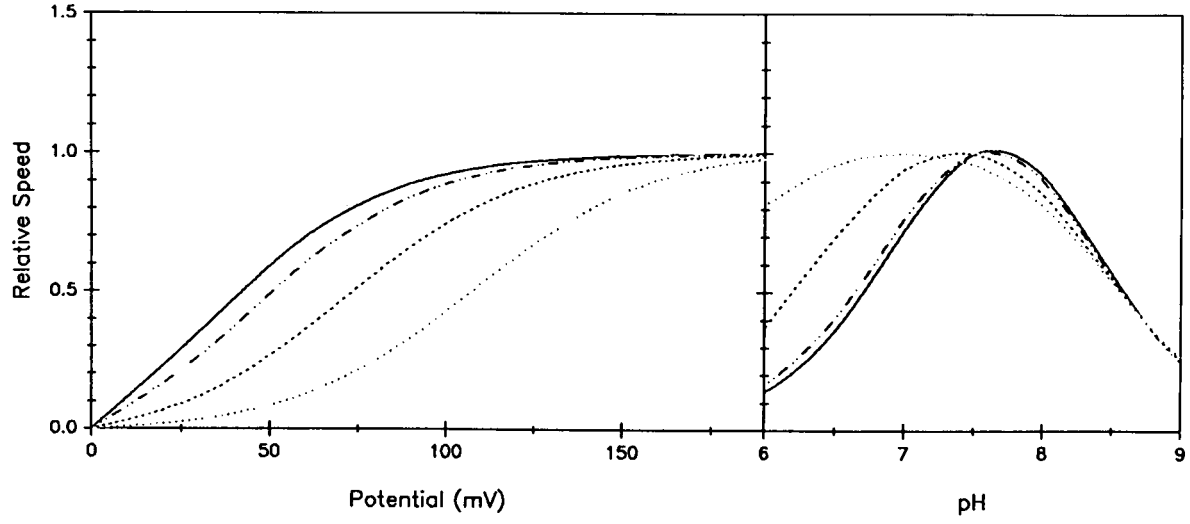


FIGURE 8 Simulation of the effect of varying $kc/(ka \cdot Kd)$ on unloaded motor speed. Potential (*right*) and pH (*left*) dependence of the unloaded motor speed at pH 7.5. $kc/(ka \cdot Kd) = 0$; $pKd = 7.0$ (——), $kc/(ka \cdot Kd) = 1$; $pKd = 7.2$ (—·—), $kc/(ka \cdot Kd) = 10$; $pKd = 7.4$ (----), $kc/(ka \cdot Kd) = 100$; $pKd = 7.5$ (·····). For each paired parameter values, speeds for each potential plot were normalized by division with the speed obtained at $-200$ mV. For each paired parameter values, speeds for each pH plot were normalized by division with the maximal speed. Based on Eq. 2.

dence of saturation on internal pH, therefore, is attenuated by increasing $kc$. At any given $Hi$, as $[kc/(ka \cdot Kd)]$ increases the zero load speed-potential curve becomes progressively sigmoidal (Fig. 8). The pH 7.5 speed-potential data are most easily accommodated by a ratio of between 1 and 10, but, as noted, possible complications due to bundle packing at very low speeds complicate interpretation of swimming cell measurements. The pH dependence of swimming speed at constant voltage (Fig. 5) indicates that $[kc/(ka \cdot Kd)]$ is unlikely to be very large (>10). Protonations/deprotonations from electronegative atoms have bimolecular rate constants between $10^{10} - 10^{11}$ $M^{-1} \cdot s^{-1}$ (Fersht, 1977). A cycle time of $10^{-4}$ s (Khan, 1988) would set a lower limit of ~1 for $[kc/(ka \cdot Kd)]$. Thus, available evidence puts $[kc/(ka \cdot Kd)]$ in the range 0.1–10.

In the limiting case where proton transfers are in rapid equilibrium, $[kc/(ka \cdot Kd)] = 0$ and Eq. 2 becomes

$$kc \cdot Kd(Ho - Hi)/2[(Kd + Ho)(Kd + Hi)]. \quad (3)$$

Because $[kc/(ka \cdot Kd)]$ ratios between 0 and 10 are discriminated poorly by the data, if at all, we will use Eq. 3 rather than Eq. 2, for ease of computation in further development of our analysis.

## Effect of load

Formulation of the work cycle as a single cycle necessitates absolute dependence of the rate of the energy coupling transition, designated as reaction (3), on the load. The free energy change, $\Delta E$, during this transition, available for work production, will be given by the Boltzmann equation: $\Delta E = RT \log \{[AH]/[BH]\}$. In the absence of an external force, $\Delta E$ will be a maximum at stall and minimum at zero load. We assume that the efficiency of the energy coupling transition is constant, independent of load and pH. The efficiency for the overall cycle (reactions [2]–[5]) will then be a function of the load, being maximum at stall.

As assumed in analyses of models for force generation in the flagellar motor (Oosawa and Hayashi, 1986; Lauger, 1988; Meister et al., 1989) and other molecular motors (Eisenberg et al., 1980), we assume that the energy barrier governing the energy coupling transition (reaction [3]) may be adequately described by transition state theory. The assumptions implicit in such a treatment have been considered by Meister et al. (1989). The free energy increase due to the mechanical work performed will affect the rate constants of the coupled transition. Though infinite possibilities exist (Hill, 1974), a commonly adopted practice is to split the free energy difference evenly between the rate constants (eg., Eisenberg et al., 1980), the most probable case. Thus,

$$k_{[AH]-[BH]} = kc \cdot \exp(-a/2)$$

$$k_{[BH]-[AH]} = kc \cdot \exp(a/2),$$

where $a = m_e/kT$, and $m_e$ is the mechanical energy per transition. Because in our single force-generator motor, one ion is transported per reaction cycle (assumption *b*), $m_e = (2\pi T/n)$, where T is the torque. Substitution into the appropriate equations for the occupational probabilities and the conservation equation in Appendix A, and solution as before, yields:

$$(dH/dt) = kc \cdot Kd \cdot [Ho \cdot e^{-(a)} - Hi]/(Z'), \quad (4)$$

where

$$(Z') = (Kd + Hi)[e^{-(a/2)} \cdot Kd + Ho \cdot e^{-(a)}] + (Kd + Ho)[e^{-(a/2)} \cdot Kd + Hi].$$

Eq. 4 may be used to derive torque frequency relations at fixed potentials or speed–potential relations at a fixed load, after the treatment by Lauger (1988). In Fig. 9 $(dH/dt)$ was scaled to $v$ by equating $(dH/dt)$ at saturating potentials with $v$ = 120 Hz (Lowe et al., 1987). $Kd$ was set to $10^{-7.0}$ M, consistent with the pH data (Fig. 8 [*right*]). For motors with multiple, independently acting force generators the stall torque, $T_m$, will be proportional to, whereas the maximal speed, $V_m$, will be independent of, the number of force generators.

The hydrodynamic drag, $\Phi$, on the cell will be $fv$ where $f$ is the frictional coefficient of the rotating cell or

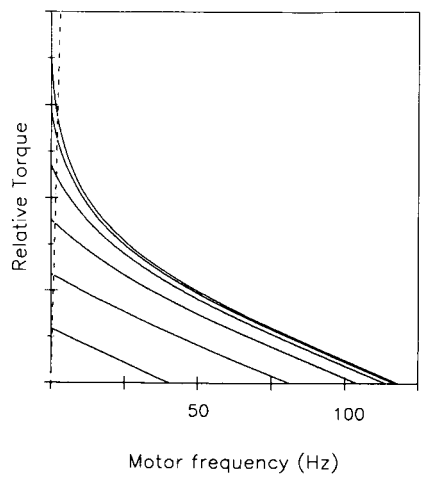


FIGURE 9 Simulations of relative motor torque versus rotation frequency at different potentials. Curves are plotted for potential increments of $\{kT/2e\}$ mV, where $e$ = unit charge; $k$ = Boltzmann's constant; $T$ = temperature. (···) = drag curve obtained for $f$ chosen to yield behavior characteristic of tethered cell rotation. Based on Eq. 4.

flagellar bundle. For a fixed $f$, the speed-potential relation may be obtained by graphical intersection of the drag curve, $\Phi = fv$, with the torque-speed relation for the various potentials (Fig. 9). Fig. 9 illustrates two important properties of a tightly coupled work cycle. First, the torque-speed relation will be a function of potential, becoming progressively linear at lower potentials. This is because $m_e$ is a function of potential as well as the number of "steps" over which work production may be partitioned (Lowe et al., 1987; Lauger, 1988). Second, the speed-potential relation will, in turn, be a function of the steady state torque, obtained upon balance of thrust and drag. The drag curve in Fig. 6 had $f$ chosen so as to intersect the torque-speed relation corresponding to a $(3kT/2e)$ mV imposed potential at 5 Hz, a rotation rate expected for a tethered cell. Such an $f$ yields a speed-potential relation consistent with that observed for tethered cells (Fig. 4 *a*). At $(3kT/2e)$ imposed potential the tethered cell torque is equivalent to the stall torque, $T_m$, within error (Meister and Berg, 1987). $T_m = \epsilon \cdot ne\Delta p/2\pi$, where $\epsilon$ is efficiency, $e$ is unit charge, and $\Delta p$ is proton potential. Given $n$ = 1,240 (Meister et al., 1987) and $\epsilon = 0.4$ (Khan, 1988), $f$ is $\sim 10^{-19}$ Js.

$f = fo + fi$, where $fo$ is the frictional coefficient due to the medium viscosity and $fi$ the intrinsic frictional coefficient of the motor. The rotation of flagellar bundles in free-swimming cells is comparable to the rotation of beads on polyhooks (Lowe et al., 1987). Thus, flagellar bundles operate under conditions where $fo \ll fi$. For $f = 0$ and $Kd = 10^{-7.0}$ M, motor frequency rises linearly then saturates ~130 mV (Fig. 9). This assumes that $fi$ is negligible, which would be the case if the membrane around the flagellum is fluid (Berg, 1974). The observed curve for swimming cells (Fig. 4 [*bottom*]), while in qualitative agreement with such predicted behavior, is nonlinear initially and saturates more gently. In *Streptococcus*, swimming speeds (>10 $\mu$m/s) may be converted to bundle rotation frequencies by multiplication with the measured proportionality constant of 6.07 $\mu m^{-1}$ (Meister, 1987), but this proportionality could alter at very low speeds due to changes in bundle packing. A significant $fi$ will account for the gentler approach to saturation. Alternatively, as considered below, saturation would be dependent on the fractional electrical distance, $d$.

## Cycle dependent changes in binding affinity

In mechanisms involving alterations of conformation (e.g., Eisenberg et al., 1980), changes in $pK$ ($-\log [Kd]$) are possible, have been argued to be kinetically favorable (Tanford, 1982), and are known to occur for some membrane transport systems and energy transducing devices (Dewey and Hammes, 1981; Tanford, 1982). To explore possible changes in the behavior of our kinetic scheme when the assumption of a single binding affinity, $Kd$, is relaxed, Eq. 2 was modified (Appendix B). Simulations of the modified equation for the pH dependence of unloaded motor speed at constant voltage are shown in Fig. 10. Fig. 10 illustrates that the maximum of the pH dependence curve will not alter regardless of the individual values of $Ka$ and $Kb$, provided that $-(pKa + pKb)/2$ is constant. Therefore, for a fixed $d$, the mean binding may be determined from the pH dependence data with accuracy regardless of possible $pK$ changes during cycling. Similarly, as indicated in Appendix B, the form of the speed potential relation will not change as a result of multiple $pK$'s.

Fig. 10 further illustrates that reversibility of the work cycle will depend on the magnitude of the binding energy changes during cycling, in addition to the load. Comparable rotation rates upon imposition of inverse proton gradients will only be obtained if $pKa$ and $pKb$ are similar. This might explain why rotation driven by inverse gradients has been obtained in some species and not in others (Ravid et al., 1986). In ATP driven motors, the substrate (ATP) and product (ADP · Pi) binding affinities are different (Eisenberg et al., 1980), which might explain why ADP · Pi have, thus far, not been shown to drive motility in vitro (Khan, 1988).

## Effect of geometry

Saturation will be a function of $Kd$ and $Hi$, hence internal pH, $H_{cyt}$. When $Ho$ tends to infinity, $(dH/dt)$ tends to $Kd/(Kd + Hi)$ (Eq. 2). Therefore, the larger the $Hi$ relative to $Kd$, the lower the saturation motor speed. For

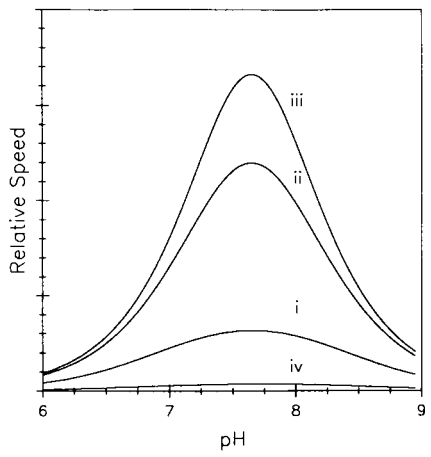


FIGURE 10 Simulation of the effect of differing $pK$'s on the pH dependence of relative unloaded speed: ($pKa$, $pKb$) were (*i*) (7, 7), (*ii*) (6, 8), (*iii*) (5, 9), (*iv*) (8, 6), respectively (see Appendix B).

any given $H_{ext}$, $H_{cyt}$, and $\Delta\Psi$; *Ho* and *Hi* will vary with *d* as follows:

$$Ho = H_{ext} \cdot e^{(-e\cdot\Delta\Psi d/kT)}$$
$$Hi = H_{cyt} \cdot e^{(e\Delta\Psi(1-d)/kT)}.$$

Because *Hi* depends on *d* as well as $H_{cyt}$, saturation will depend on *d*. In contrast, when a $\Delta$pH is imposed, $Ho = H_{ext}$ and $Hi = H_{cyt}$. Therefore, the kinetic equivalence of $\Delta\Psi$ and $\Delta$pH in affecting the unloaded speed, as well as the pH dependence of saturation speed, would depend on *d*. Note that the stall torque will be independent of *d* because $[\log (Ho/Hi)] = [-(e\Delta\Psi/kT) + \log (H_{ext}/H_{cyt})]$.

We incorporate the above equations for the local activities into Eq. 3. This yields

$$(dH/dt) = kc \cdot Kd' \cdot \{H_{ext} \cdot e^{[-e\cdot\Delta\Psi d/kT]} - H_{cyt} \cdot e^{[e\Delta\Psi(1-d)/kT]}\}/(Z''), \quad (5)$$

where

$$Kd' = Kd \cdot e[-e \cdot (1 - d)/kT]$$
$$(Z'') = 2 \cdot [Kd' + H_{ext} \cdot e^{(-e\cdot\Delta\Psi d/kT)}] \cdot [Kd' + H_{cyt} \cdot e(e\Delta\Psi(1-d)/kT].$$

As proven in Appendix C, adjustment of the binding constant, *Kd*, in Eq. 3 to $Kd \cdot \exp[-e \cdot \Delta\Psi(1 - d)/kT]$ will allow fit of the pH dependence data regardless of *d*. However, once *Kd* is thus fixed, the speed potential data at pH 6.25 versus 8.75 as well as the $\Delta\Psi/(2.3\ RT/F)\Delta$pH equivalence at pH 8.75 provide strong discrimination among possible *d* values, as appreciated by consideration of Fig. 6. The form of the dependence of saturation on pH and $\Delta\Psi/(2.3\ RT/F)\Delta$pH equivalence at pH 8.75 is attenuated, but not appreciably when $(kc/ka \cdot Kd) = 10$ (simulations not shown). Such attenuation, if not taken into account as in Fig. 11, will result in underestimates of *d*. We conclude that the groups that participate in the reactions limiting motor speed have an electrical distance extending between three-fourths to all of the way across the membrane toward the cytoplasm. Accordingly, the mean *pK* of these groups is estimated to range between 7.325 ($d = 3/4$) and 7.0 ($d = 1$).

One implication of Fig. 7 is that only the reactions that occur at the energy coupling sites ([2]–[5]) are voltage insensitive. Clearly reactions (1) and (6) may be decomposed into many reactions, some of which, such as initial binding of bulk phase protons to the membrane channels, will be voltage insensitive. These might be rate-limiting, though the particular case of bulk-phase proton transfers would be expected to be fast, due to buffering (Fersht, 1977). However, the speed–potential relation in tethered cells is modulated similarly by pH (Fig. 6 [*top left; top right*]), as that in swimming cells (Fig. 6 [*bottom left; bottom right*]), though attenuated due to the higher load. This suggests the participation of the energy coupling sites in the reactions limiting motor speed. In the high load regime encountered in tethered cells, the energy coupling transition (reaction [3]) will be rate limiting. If other reactions on groups spatially removed from the energy coupling sites were to limit cycling in the low load regime encountered in swimming cells, such similarity could not be easily explained. Finally, if the energy coupling sites occur outside of the transmembrane electric field (e.g., in the cytoplasm) as the data imply, this obviates special stereochemical constraints for explanation of the voltage insensitivity (Fig. 7 legend).

## DISCUSSION

Two criteria define a tightly coupled motor: (*a*) the stall torque of the motor must be proportional to the applied potential and (*b*) the ion flux through the motor must be proportional to its rotation frequency. To assess tightness of coupling in the flagellar motor as determined by the first criterion, we have drawn upon and extended contributions from earlier studies (Manson et al., 1980; Khan and Berg, 1983; Conley and Berg, 1984; Khan, Meister, and Berg, 1985; Meister and Berg, 1987). These studies had shown that artificially energized tethered cell rotation increased linearly with potential up to −85 mV (Khan et al., 1985). Changes in glycolyzing cell rotation as a function of external pH were most simply interpreted as indicative of a linear speed-potential relation (Manson et al., 1980). But this could not be unambiguously determined in the absence of potential measurements because the interpretation assumed constant internal pH and membrane potential over the range investigated. Bacteria maintain pH homeostasis over a wide range of external pH; but while some maintain membrane potential constant over the range (Ramos et al., 1976), others do not (Khan and Macnab, 1980). Our potential measurements confirm the interpretation of Manson et al. (1980) and show that right up to the highest potentials accessible to investigation, ~−200 mV, the relation remains close to linear. Because tethered cell rotation has been shown to track stall torque throughout this range (Meister and Berg, 1987), this implies that the stall torque is proportional to the applied potential. As Fig. 9 illustrates, it would be expected that the discrepancy between stall torque and tethered cell running torque increase at higher potentials. The slight curvature observed in the data of Fig. 4 (*top*) could be the result of this difference.

Measurements of swimming speed as a function of

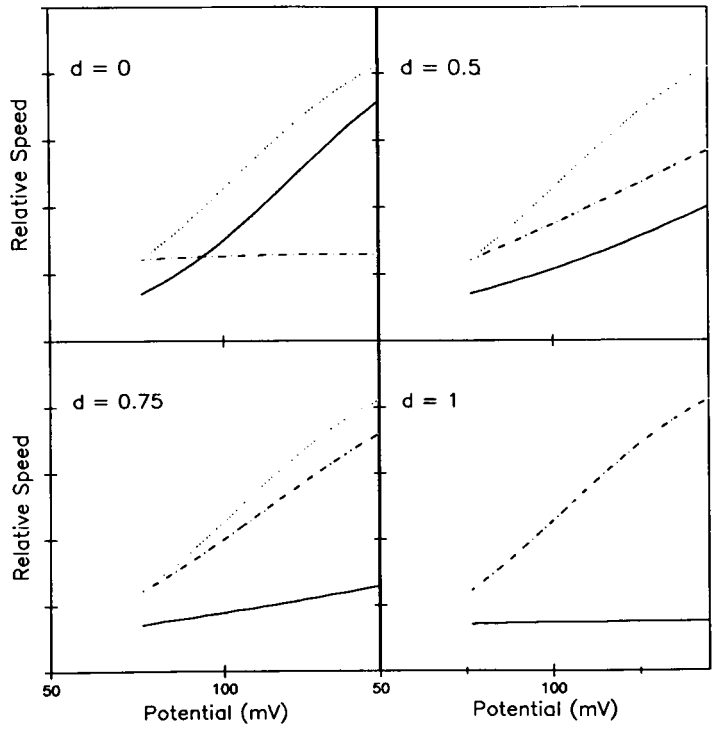


FIGURE 11 Potential dependence and $\Delta\Psi - (2.3\ RT/F)$ pH equivalence of unloaded speed as a function of fractional electrical distance. $pKd$ = 8.3, 7.65, 7.325, and 7.0 for fractional electrical distance, $d$ = 0, 0.5, 0.75, and 1, respectively, (see Appendix C). Internal pH 6.25 (——). Internal pH 8.75; energization by $\Delta\Psi$ (—·—). Internal pH 8.75; energization by (2.3 $RT/F$) pH atop a base potential of −76.5 mV $\Delta\Psi$ (·····). For $d$ = 1, (—·—) and (·····) are superimposed. Based on Eq. 5.

potential had not been made previously for *Streptococcus*. We were motivated to make these measurements by the work of Lowe et al. (1987) which established that flagellar motors in a swimming cell bundle, in contrast to a tethered cell, operate at negligible load. Our observations of the relation between swimming speed and potential are similar to that obtained in *B. subtilis* (Khan and Macnab, 1980; Shioi et al., 1980). They agree well with the data of Shioi et al. (1980), the data of Khan and Macnab (1980) now being known to be flawed by erroneous estimates of the membrane potential (Zaritsky et al., 1981). The linearization of the saturation regime as the load is increased by changing from swimming to tethered cell geometry would be explicitly predicted by, and provides support for, tight coupling. In the work of Shioi et al. (1980) the differences between tethered and free-swimming cells could have been missed given culture to culture variation. Further, for *B. subtilis*, it is not known how torque and rotation in tethered and free-swimming cells relate to the maximal torque and rotation. Thus, coupling as assessed by criterion (*a*), seems to be remarkably tight. As regards criterion (*b*), whereas assays for measurement of total flux remain to be devised, Meister et al. (1987) have shown that the rotation coupled motor flux is proportional to rotation frequency. The body of evidence that may be marshalled in support of tight coupling is becoming impressive.

The comparison of glycolyzing and artificially energized motility is of significance in the context of possible involvement of local circuits (Williams, 1988), an argument that has been made for other chemiosmotic devices. The potential measurements, for the first time, allow detailed comparison between artificially energized and metabolizing cells. The case for local circuits in energization of the flagellar motor is not persuasive (Fig. 4). However, more refined measurements will need to be made to rule out local circuits.

An important consensus result of the studies on swimming cells, including the present one, is that speed saturates regardless of whether the electrical or chemical potential components of the proton potential are incremented. Further, the saturation speed is the same in both cases. The equivalence of $\Delta\Psi$ and (2.3 $RT/F$)$\Delta$pH will depend on whether the voltage insensitive or voltage sensitive reactions are rate limiting. Analysis of saturation of the swimming speed-potential relation as a func-

tion of load, pH, and composition of the driving potential has yielded estimates of the electrical distance, $d$, and mean proton binding affinity of the groups that participate in the voltage insensitive rate limiting reactions. We have argued that these groups are, in fact, the energy coupling sites.

The "robustness" of our estimates depends on the assumptions inherent in our kinetic analysis. We have endeavoured to make these assumptions explicit. Many of these assumptions have been used in recent analyses of motor models (Oosawa and Hayashi, 1986; Lauger, 1988; Meister et al., 1989). However, the specific model dependent postulates in these analyses regarding force-generation geometry (eg., "crossed channels" [Lauger, 1988]) and mechanism (eg., "drift of half-channels coupled to stretch of elastic linkages" [Meister et al., 1989]) are not required for interpretation of our steady state data. For example, the equivalence of $\Delta\Psi$ and $(2.3\ RT/F)\Delta$pH in driving unloaded motor rotation will depend strongly on the electrical distance, regardless of molecular details of the energy coupling. Alternatively stated, our data cannot be used to discriminate between motor models. Currently viable models are reviewed by Khan (1990).

Our analysis bears similarity to the analyses found in the electrophysiological literature for estimation of the electrical distance of ion channel blockage sites (Woodhull, 1973; Coronado et al., 1980). The key assumption in these analyses, analogous to the assumption of tight coupling made here, is that blockage is absolute (Yellen, 1987). The correspondence of electrical distance with physical distance will depend on the profile of the electric field within the membrane. For a constant electric field, an assumption often made (Junge, 1981), the correspondence will be exact. However, at least in the case of the sarcoplasmic reticulum $K^+$ channel a substantial fraction of the voltage drop is experienced a few angstroms within the membrane (Miller, 1982).

It is of interest to compare our findings with similar studies in other chemiosmotic devices. In studies of the *Streptococcus* ATPase, Maloney and Schattschneider (1980) imposed artificial $\Delta\Psi$ and $\Delta$pH gradients and found that until nominal values of $\sim -300$ mV, these had equivalent weight in driving ATP synthesis. This evidence is, and was, most simply interpreted in terms of a proton well ($d = 1$) consistent with known structural and enzymological evidence, namely that the $F_1$ ATPase is located in the cytoplasm and that product release limits cycling (Maloney, 1982). In the case of the flagellar motor, the location of the energy transducing sites and the nature of the events limiting unloaded motor rotation remain unknown. Thus, this study provides novel information which should spur chemical and structural investigations of the flagellar motor.

## APPENDIX A

## Rate equation for the motor cycle

The steady-state occupational probabilities of the cycling forms will be given by four linear equations:

$$d[A]/dt = kc \cdot [B] + ka \cdot Kd[AH] - (kc + ka \cdot Ho) \cdot [A] = 0$$

$$d[B]/dt = kc \cdot [A] + ka \cdot Kd[BH] - (kc + ka \cdot Hi) \cdot [B] = 0$$

$$d[AH]/dt = ka \cdot Ho[A] + kc \cdot [BH] - (kc + ka \cdot Kd) \cdot [AH] = 0$$

$$d[BH]/dt = ka \cdot Hi[B] + kc \cdot [AH] - (kc + ka \cdot Kd) \cdot [BH] = 0.$$

This system of equations together with the conservation equation

$$[A] + [B] + [AH] + [BH] = 1$$

allows a unique solution of the steady-state occupation probabilities by either elimination or matrix inversion (Kreysig, 1983). The flux, $(dH/dt)$, may be obtained by substitution into any of the flux equations below.

$$\begin{aligned}(dH/dt) &= kc \cdot ([AH] - [BH]) \\ &= kc \cdot ([B] - [A]) \\ &= ka \cdot (Ho \cdot [A] - Kd \cdot [AH]) \\ &= ka \cdot (Kd \cdot [BH] - Hi \cdot [B]).\end{aligned}$$

Thus,

$$(dH/dt) = kc \cdot (Ho - Hi)/2(Z), \qquad (3)$$

where

$$\{Z\} = \{(Kd + Ho)(Kd + Hi)/Kd\} + (kc/ka \cdot Kd)\{2 \cdot Kd + Ho + Hi\}.$$

## APPENDIX B

## *pK* changes during cycling

The configurational transitions of the work cycle may involve conformational changes with attendant alteration in binding affinities. Eisenberg et al. (1980) provide a detailed treatment of this point. For simulation of such cases, we replace $Kd$ by two binding constants characteristic of each configuration, $Ka$ and $Kb$. At chemical equilibrium ($Ho = Hi$; $[dH/dt] = 0$), each of the individual reactions, including (2) and (4) (Fig. 7), will be at equilibrium. Therefore,

$$[AH]_{eq} = [A]_{eq} \cdot H/Ka$$

$$[BH]_{eq} = [B]_{eq} \cdot H/Kb,$$

where $[A]_{eq}$, $[B]_{eq}$, $[AH]_{eq}$, and $[BH]_{eq}$ are the equilibrium occupational

probabilities. Therefore,

$$\{[AH]_{eq}/[BH]_{eq}\}\{[B]_{eq}/[A]_{eq}\} = (Kb/Ka).$$

We assume, as before, that the free energy change will be the same for transitions between the protonated or unprotonated configurations. However, because $(Kb/Ka)$ is not unity, this free energy change will not be zero. Now

$$RT \cdot \log([AH]_{eq}/[BH]_{eq}) = RT \cdot \log([B]_{eq}/[A]_{eq}) = 0.5 \cdot \log(Kb/Ka).$$

Again, as for analysis of the effect of load, we split the free energy change during the transitions $[AH]$ to $[BH]$ and $[B]$ to $[A]$ equally between the rate constants. Thus,

$$k_{[AH]-[BH]} = kc \cdot (Kb/Ka)^{-0.25}$$
$$k_{[BH]-[AH]} = kc \cdot (Kb/Ka)^{0.25}$$
$$k_{[A]-[B]} = kc \cdot (Kb/Ka)^{-0.25}$$
$$k_{[B]-[A]} = kc \cdot (Kb/Ka)^{0.25}.$$

Substitution of these rate constants into the equations for the occupational probabilities and the conservation equation in Appendix A and solution as before for the flux $(dH/dt)$ at zero load, yields

$$(dH/dt) = kc \cdot Ka \cdot (Ho - Hi)/(Z'),$$

where

$$\{Z'\} = (Kb + Hi)\{Ka + [Ho \cdot (Kb/Ka)^{-0.5}]\} + (Ka + Ho)\{Hi + [Kb \cdot (Kb/Ka)^{-0.5}]\}.$$

When $Ho$ is large, the flux tends to $kc \cdot Ka/\{(Hi \cdot (1 + (Kb/Ka)^{-0.5})) + (2 \cdot Kb \cdot (Kb/Ka)^{-0.5})\}$. Thus pH dependence of saturation of the same form as that predicted by Eq. 3 is obtained.

## APPENDIX C

## The form of the pH dependence at constant voltage is independent of electrical distance

Let $c = -e\Delta\Psi/kT$ and $Hi = H_{cyt} = H_{ext}$. Then Eq. 5 becomes

$$(dH/dt) = kc \cdot Kd' \cdot Hi[e^{cd} - e^{-c(1-d)}]/2 \cdot \{[Kd' + Hi \cdot e^{cd}][Kd' + Hi \cdot e^{-c(1-d)}]\}.$$

Substitution of $Kd \cdot e^{-c(1-d)}$ for $Kd'$ into the above equation will remove the $d$ dependence for a given $c$ and establish identity of Eq. 5 with Eq. 3. Consider the right hand side of the equation, with $(kc/2)$ factored out. Upon substitution, factorization of $e^{-c(1-d)}$ from both numerator and denominator and cancellation we get

$$Kd \cdot Hi[e^{cd} - e^{-c(1-d)}]/\{[Kd \cdot e^{-c(1-d)} + Hi \cdot e^{cd}][Kd + Hi]\}.$$

Upon factorization of $e^{cd}$ from both numerator and denominator and cancellation we get

$$Kd \cdot Hi(1 - e^{-c})/[(Kd \cdot e^{-c} + Hi)(Kd + Hi)] = Kd \cdot Hi(e^{c} - 1)/[(Kd + Hi \cdot e^{c})(Kd + Hi)] = Kd \cdot (Ho - Hi)/[(Kd + Ho)(Kd + Hi)].$$

We are grateful to Dr. H. R. Kaback for the gift of $H^3$-tetraphenylphosphonium. We thank Drs. M. Meister, R. Caplan, and H.C. Berg for sharing the results of their analysis with us before publication and Drs. H. Morowitz and J. Segall for comments on the manuscript.

This work was supported by National Institutes of Health grant 36936.

*Received for publication 25 April 1989 and in final form 30 November 1989.*

## REFERENCES

Bakker, E. P., and W. E. Mangerich. 1981. Interconversion of components of the bacterial proton motive force by electrogenic potassium transport. *J. Bacteriol.* 147:820–826.

Berg, H. C. 1974. Dynamic properties of bacterial flagellar motors. *Nature (Lond.).* 249:77–79.

Berg, H. C., and R. A. Anderson. 1973. Bacteria swim by rotating their flagellar filaments. *Nature (Lond.).* 245:380–382.

Berg, H. C., and S. M. Block. 1984. A miniature flow-cell designed for rapid exchange of media under high-power objectives. *J. Gen. Microbiol.* 130:2915–2920.

Berg, H. C., and S. Khan. 1983. A model for the flagellar rotary motor. *In* Mobility and Recognition in Cell Biology. H. Sund and C. Veeger, editors. De Gruyter, Berlin. 485–497.

Berg, H. C., and L. Turner. 1979. Movement of microorganisms in viscous environments. *Nature (Lond.).* 278:349–351.

Berg, H. C., M. D. Manson, and P. Conley. 1982. Dynamics and energetics of flagellar rotation in bacteria. *Symp. Soc. Exp. Biol.* 35:1–31.

Blair, D., and H. C. Berg. 1988. Restoration of torque in defective flagellar motors. *Science (Wash. DC).* 242:1678–1681.

Conley, P., and H. C. Berg. 1984. Chemical modification of *Streptococcus* flagellar motors. *J. Bacteriol.* 158:832–843.

Cooke, R., and W. Bialek. 1979. Contraction of glycerinated muscle fibres as a function of the ATP concentration. *Biophys. J.* 28:241–258.

Coronado, R., R. L. Rosenberg, and C. Miller. 1980. Ionic selectivity, saturation and block in a $K^+$ channel from sarcoplasmic reticulum. *J. Gen. Physiol.* 76:425–446.

DePamphilis, M., and J. Adler. 1971. Purification of intact flagella from *Escherichia coli* and *Bacillus subtilis*. *J. Bacteriol.* 105:376–383.

Dewey, T. G., and G. G. Hammes. 1981. Steady state kinetics of ATP synthesis and hydrolysis catalyzed by reconstituted chloroplast coupling factor. *J. Biol. Chem.* 10:8941–8946.

Dibrov, P. A., V. A. Kostyrko, R. L. Lazarova, V. P. Skulachev, and I. A. Smirnova. 1986. The sodium cycle. I. $Na^+$ dependent motility and modes of energization in the marine alkalotolerant *Vibrio alginolyticus*. *Biochem. Biophys. Acta.* 850:449–457.

Dimmit, K., and M. Simon. 1971. Purification and thermal stability of intact *Bacillus subtilis* flagella. *J. Bacteriol.* 105:369–375.

Eisenberg, E., T. L. Hill, and Y.-D. Chen. 1980. Cross-bridge model of muscle contraction. Quantitative analysis. *Biophys. J.* 29:195–227.

Fersht, A. 1977. Enzyme Structure and Mechanism. W. H. Freeman and Co.

Guffanti, A. A., S. Clejan, L. H. Falk, D. B. Hicks, and T. A. Krulwich. 1987. Isolation and characterization of uncoupler resistant mutants of *Bacillus subtilis*. *J. Bacteriol.* 169:4469–4478.

Hill, T. L. 1974. Theoretical formalism for the sliding filament model of contraction of striated muscle. Part I. *Prog. Biophys. Mol. Biol.* 269–339.

Hill, T. L. 1977. Free Energy Transduction in Biology. Academic Press, Inc., New York.

Hirota, N., and Y. Imae. 1983. $Na^+$ driven flagellar motors of an alkalophilic Bacillus strain YN-1. *J. Biol. Chem.* 258:10577–10581.

Junge, D. 1981. Nerve and muscle excitation. Sinauer Associates, Inc., Sunderland, MA.

Kashket, E. 1985. The proton motive force in bacteria: a critical assessment of methods. *Annu. Rev. Microbiol.* 39:219–242.

Kashket, E., and S. L. Barker. 1977. Effects of potassium ions on the electrical and pH gradients across the membranes of *Streptococcus lactis* cells. *J. Bacteriol.* 130:1017–1023.

Khan, S. 1980. Ph.D. thesis. Energetics of bacterial motility. Yale University, New Haven, CT.

Khan, S. 1988. Analysis of bacterial flagellar rotation. *Cell Motil. Cytoskeleton.* 10:38–46.

Khan, S. 1990. Motility. *In* The Bacteria: a Treatise on Structure and Function. Vol XII. I. C. Gunsalus, J. R. Sokatch, and L. N. Ornsdon, editors. Academic Press, Inc., New York. In press.

Khan, S., and H. C. Berg. 1983. Isotope and temperature effects in chemiosmotic coupling to the flagellar motor of *Streptococcus. Cell.* 32:913–919.

Khan, S., and R. M. Macnab. 1980. Proton chemical potential, proton electrical potential and bacterial motility. *J. Mol. Biol.* 138:599–614.

Khan, S., M. Meister, and H. C. Berg. 1985. Constraints on flagellar rotation. *J. Mol. Biol.* 184:645–656.

Khan, S., M. Dapice, and T. S. Reese. 1988. Effects of *mot* gene expression on the structure of the flagellar motor. *J. Mol. Biol.* 202:575–584.

Kihara, M., and R. M. Macnab. 1981. Cytoplasmic pH mediates pH taxis and weak-acid repellent taxis of bacteria. *J. Bacteriol.* 140:297–300.

Kreysig, E. 1983. Advanced Engineering Mathematics. John Wiley and Sons, Inc., New York.

Lauger, P. 1977. Ion transport and rotation of bacterial flagella. *Nature (Lond.).* 268:360–362.

Lauger, P. 1988. Torque and rotation rate of the bacterial flagellar motor. *Biophys. J.* 53:53–66.

Lowe, G., M. Meister, and H. C. Berg. 1987. Rapid rotation of flagellar bundles in swimming bacteria. *Nature (Lond.).* 325:637–640.

Macnab, R. M., and D. DeRozier. 1988. Bacterial flagellar structure and function. *Can. J. Microbiol.* 34:452–441.

Maloney, P. 1982. Energy coupling to ATP synthesis by the proton translocating ATPase. *J. Memb. Biol.* 67:1–12.

Maloney, P., and S. Schattschneider. 1980. Voltage sensitivity of the proton-translocating adenosine 5'-triphosphatase in *Streptococcus lactis. FEBS (Fed. Eur. Biochem. Soc.) Lett.* 110:337–340.

Manson, M. D., P. Tedesco, H. C. Berg, F. M. Harold, and C. van der Drift. 1977. A protonmotive force drives bacterial flagella. *Proc. Natl. Acad. Sci. USA.* 74:3060–3064.

Manson, M., P. Tedesco, and H. C. Berg. 1980. Energetics of flagellar rotation in bacteria. *J. Mol. Biol.* 138:541–561.

Meister, M. 1987. Ph.D. thesis. Studies of flagellur rotation: the angular symmetry, the stall torque, and the proton consumption of the bacterial flagellar motor. California Institute of Technology, Pasadena, CA.

Meister, M., and H. C. Berg. 1987. The stall torque of the bacterial flagellar motor. *Biophys. J.* 52:413–419.

Meister, M., G. Lowe, and H. C. Berg. 1987. The proton flux through the bacterial flagellar motor. *Cell.* 49:643–650.

Meister, M., R. Caplan, and H. C. Berg. 1989. Dynamics of a tightly coupled model for flagellar rotation. *Biophys. J.* 55:905–914.

Miller, C. 1982. Bis-quaternary ammonium blockers as structural probes of the sarcoplasmic reticulum $K^+$ channel. *J. Gen. Physiol.* 79:869–891.

Mitchell, P. 1984. Bacterial flagellar motors and osmoelectric molecular rotation by an axially transmembrane well and turnstile mechanism. *FEBS (Fed. Eur. Biochem. Soc.) Lett.* 176:289–294.

Oosawa, F., and S. Hayashi. 1986. The loose coupling mechanism in molecular machines of living cells. *Adv. Biophys.* 22:151–183.

Oosawa, F., and J. Masai. 1982. Mechanism of flagellar motor rotation in bacteria. *J. Physiol. Soc. Jpn.* 51:631–641.

Ramos, S., S. Schuldiner, and H. R. Kaback. 1976. The electrochemical gradient of protons and its relationship to active transport in *Escherichia coli* membrane vesicles. *Proc. Natl. Acad. Sci. USA.* 73:1892–1896.

Ravid, S., P. Matsumura, and M. Eisenbach. 1986. Restoration of flagellar clockwise rotation in bacterial envelopes by insertion of the chemotaxis protein Che Y. *Proc. Natl. Acad. Sci. USA.* 83:7157–7161.

Shioi, J-I., P. Matsuura, and Y. Imae. 1980. Quantitative measurements of protonmotive force and motility in *Bacillus subtilis. J. Bacteriol.* 144:891–897.

Stewart, R. C., and F. W. Dahlquist. 1987. Molecular components of bacterial chemotaxis. *Chem Rev.* 87:997–1025.

Sugiyama, S., E. J. Cragoe, Jr., and Y. Imae. 1988. Amiloride, a specific inhibitor for the $Na^+$-driven flagellar motors of alkalophilic bacillus. *J. Biol. Chem.* 263:8215–8219.

Sundberg, S. A., M. Alam, and J. L. Spudich. 1986. Excitation signal processing times in *Halobacterium halobium* phototaxis. *Biophys. J.* 50:895–900.

Tanford, C. 1982. Steady state of an ATP-driven calcium pump: limitations on kinetic and thermodynamic parameters. *Proc. Natl. Acad. Sci. USA.* 79:6161–6165.

Tanford, C. 1983. Mechanism of free energy coupling in active transport. *Annu. Rev. Biochem.* 52:379–409.

Tokuda, H., and T. Unemoto. 1982. Characterization of the respiration-dependent $Na^+$ pump in the bacterium *Vibrio alginolyticus. J. Biol. Chem.* 257:10007–10014.

Williams, R. J. P. 1988. Proton circuits in biological energy interconversions. *Annu. Rev. Biophys. Biophys. Chem.* 17:71–98.

Woodhull, A. M. 1973. Ionic blockage of sodium channels in nerve. *J. Gen. Physiol.* 61:687–708.

Yellen, G. 1987. Permeation in potassium channels: implications for channel structure. *Annu. Rev. Biophys. Biophys. Chem.* 16:227–246.

Zaritsky, A., M. Kihara, and R. M. Macnab. 1981. Measurement of membrane potential in *Bacillus subtilis:* a comparison of lipophilic cations, rubidium ion and a cyanine dye as probes. *J. Membr. Biol.* 63:215–231.